Acoustical Zone Reproduction for Car Interiors Using a MIMO MSE Framework

Simon Berthilsson[1,2], Annea Barkefors[1,2], Lars-Johan Brännmark[1,2] and Mikael Sternad[1,2]

[1]*Signals and Systems, Uppsala University, Box 534, 751 21 Uppsala, Sweden.*

[2]*Dirac Research AB, Uppsala, Sweden.*

Correspondence should be addressed to Simon Berthilsson (simon.berthilsson@signal.uu.se)

ABSTRACT

The problem of dividing the listener space of a commercial series-production car into several acoustical zones is examined. The sound of each zone is to be isolated from the sounds of the other zones and may consist of e.g. music or speech. A solution is proposed where the low frequency part of the problem is solved by the installed entertainment system speakers and the higher frequency part of the problem is solved by inexpensive local speakers. This paper focuses on the low frequency part of the problem and presents a solution that generates a sound pressure difference between all zones in excess of 10 dB for most frequencies in the range 70–400 Hz for an example problem.

1. INTRODUCTION

Soundfield reproduction over extended areas of space has been under study for some time now. While most efforts focus on reproducing a single soundfield, a few papers have also been published with the aim of creating several zones of different acoustical characteristics, see e.g. [1] and [2]. The main benefit of acoustical zones is the possibility to create personalized audio without the need for headphones. This in turn results in increased listener comfort and added safety by allowing external warning noises to be heard more freely. This paper focuses on an implementation in a car, a space that is often shared among several different users with varying desires and demands on the audio system. The easiest and most straightforward way of rendering acoustical zones is to use loudspeakers located close to the listeners. This allows for low output power to produce satisfactory sound levels around the targeted listener while still being barely audible a small distance away. A refined take on this approach is investigated in [3]. The main drawback of such a system is the price of speakers that have good enough bass reproduction while being small enough to be fitted in the headrests or ceiling of a car in a non intrusive way. Using the speakers that are readily available in mid- and high-end car audio systems of today to generate the zones is a cheaper option but the limited number of loudspeakers makes soundfield reproduction at high frequencies infeasible (see e.g. [4]). We here suggest a hybrid system where the lower frequencies are dealt with by the traditional loudspeaker system and higher frequencies are supported by cheaper speakers fitted in the headrests or the ceiling, close to the respective listener.

This paper will explore the low frequency part of such a system. A multipoint Mean Square Error (MSE) feedforward control strategy based on LQG or H_2 optimal control will be employed to control the soundfield. The controller filters are designed using a polynomial approach [5] which provides increased structural insight and good numerical properties as compared to state-space methods. The design method also avoids inversion of large block-Toepliz matrices as is the case with time domain matrix-based MSE methods (see e.g. [6]). The polynomial design constitutes a special case of a more general design derived in [7]. This method has previously been successfully used in soundfield control problems [8] and is used as a unified solution to the problem of equalizer design, crossover design, delay and level calibration, sum-response optimization and up-mixing in car audio systems [9]. It has recently been applied also to active noise control problems [10]. The MSE approach also has the desirable properties that it is not based on any hard-to-fulfil physical assumptions and that it uses a time domain criterion, allowing an explicit constraint on causality to be included in the design. A different ap-

proach, described in [2] produces impressive results but rely on absolute freedom to choose loudspeakers and also require one loudspeaker per targeted point. Yet another approach is considered in [1], where spherical harmonics are used with some promising results.

The paper is structured as follows: In Section 2, the theoretical framework is sketched. Section 3 describes the experimental set-up and contains the experimental results. Section 4 holds a discussion of the results and conclusions.

1.1. Notation

The trace and transpose of a matrix $\mathbf{M}$ are denoted $\mathrm{tr}\mathbf{M}$ and $\mathbf{M}'$, respectively. Causal and time-invariant FIR filters with real-valued coefficients $\{p_n\}$ are here represented by polynomials in the backward time shift operator q^{-1}

$$P(q^{-1}) = p_0 + p_1 q^{-1} + \ldots + p_{np} q^{-np} \ ,$$

where $v(t-1) = q^{-1}v(t)$ while $v(t+1) = qv(t)$ for discrete-time signals $v(t)$. Polynomial matrices have FIR filters as elements. They are represented by bold italics, $\boldsymbol{P}(q^{-1})$. A square polynomial matrix $\boldsymbol{P}(q^{-1})$ is denoted *stable* if all zeros of $\det[\boldsymbol{P}(z^{-1})]$ are located in $|z| < 1$. For a polynomial matrix $\boldsymbol{P}(q^{-1})$, the corresponding *conjugate matrix* $\boldsymbol{P}_*(q)$ is defined as its conjugate transpose, with the forward shift operator q substituted for q^{-1} as argument in all polynomials.

Rational matrices have discrete-time rational transfer operators as elements. They are denoted by bold calligraphic symbols such as $\boldsymbol{\mathscr{R}}(q^{-1})$. Arguments ($q^{-1}, q, z^{-1}$ or z) are omitted where there is no risk of misunderstanding. A rational matrix may be parameterized in terms of polynomial matrices as a matrix fraction description (MFD), either left MFD $\boldsymbol{\mathscr{R}} = \boldsymbol{A}_1^{-1}\boldsymbol{B}_1$ or right MFD $\boldsymbol{\mathscr{R}} = \boldsymbol{B}_2\boldsymbol{A}_2^{-1}$ (see e.g. Ch. 6 of [11]).

2. MIMO LQG FEEDFORWARD SOUNDFIELD CONTROL

A linear acoustic system consists of M control points (measurement positions) and N actuating loudspeakers. The control points may be partitioned into g groups, $G_1, ..., G_g$. The microphones used to estimate the acoustic transfer functions to the control points are assumed to be spaced by no more than the spatial Nyquist sampling distance within each group for the highest frequency to be controlled. In the present case, the spacing is 0.1 m yielding an upper frequency limit of 1700 Hz for control within each group. These groups will represent the acoustical zones in our framework. The space that is not included in any group is viewed as a 'don't care' zone and the soundfield in this area is not actively controlled.

The total control system is here designed as a superposition of g feedforward control algorithms that each produce a desired soundfield in one or several of the zones, denoted the target group G_T, and silence in the remaining zones. Each of these g control systems is fed by L signals $r_p(t)$, with elements represented by column vectors $r_{\ell,p}(t), \ell = 1,\ldots,L, p = 1,\ldots,g$. The vector $r_p(t)$ represents the sound channels used in the zone or zones targeted by controller p. The use of $L = 2$ could e.g. represent a stereo system with appropriate staging, virtual source location and redesigned room acoustic response [9]. The L-channel sound could be generated by several audio signals, e.g. music, telephone calls or the navigation system. The total output signal to the loudspeakers may be regarded as a superposition of the signals that each group wishes to listen to, filtered through the controller filters for the respective target group.

2.1. Model Parameterizations

The acoustic channels from the N control loudspeakers to the M measurement positions, including transport delays, need to be measured and modeled. The sampled sound signal at the measurement positions, $y(t)$, is described by an $M \times 1$ column vector and is modeled by

$$y(t) = \boldsymbol{\mathscr{H}}(q^{-1})u(t) = \boldsymbol{B}(q^{-1})\boldsymbol{A}^{-1}(q^{-1})u(t) \ . \quad (1)$$

Here, the $N \times 1$ column vector $u(t)$ represents the loudspeaker input signals at discrete time t. The $M \times N$ polynomial matrix $\boldsymbol{B}(q^{-1})$ and the $N \times N$ stable polynomial matrix $\boldsymbol{A}(q^{-1})$ constitute a right MFD representation of the dynamics. For FIR models, which we will employ throughout this paper, $\boldsymbol{A}(q^{-1}) = \mathbf{I}$.

The desired transfer functions from the sampled sound signals $r_p(t)$ to the measurement positions are modeled by an $M \times L$ matrix of FIR filters, $\boldsymbol{D}(q^{-1})$. This model describes all desired effects of the reconstruction, sound propagation, sampling and anti aliasing filtering. Thus, the desired sound at the measurement positions, $z(t)$, may be represented by

$$z(t-d) = q^{-d}\boldsymbol{D}(q^{-1})r_p(t) \ . \quad (2)$$

A natural choice for a zone design is to set the rows of $\boldsymbol{D}(q^{-1})$ equal to one for the positions corresponding to G_T, aiming at a flat magnitude spectrum, and zero for the other rows. Other meaningful choices are possible. For instance, by setting progressively longer delays of the ones in the rows of $\boldsymbol{D}(q^{-1})$, a staging effect can be achieved for one of the L sound channels, creating a virtual source location.

The factor q^{-d} is introduced as a means of setting a common delay to all target positions and may be viewed as the greatest common delay of all desired transfer functions. The discrete-time delay, d in (2) needs to be at least equal to the transportation delay between any measurement point and the closest loudspeaker (minus any delays incorporated in $\boldsymbol{D}(q^{-1})$). If this is not fulfilled we are asking the sound waves produced by the system to act upon the measurement grid before it is physically possible to do so, with decreased performance as a result.

If some spectral properties of $r_p(t)$ are known, they may be included in the solution by representing them by a stable vector-autoregressive model

$$\boldsymbol{H}(q^{-1})\, r_p(t) = e(t) \quad , \tag{3}$$

where $e(t)$ is a zero mean discrete-time white noise sequence with covariance matrix $\mathbf{R}_e$.

2.2. The Design Problem

The LQG feedforward controller for a target group may now be defined as

$$u(t) = \boldsymbol{\mathscr{R}}_p(q^{-1})\, r_p(t+d) \ . \tag{4}$$

Further, we define the corresponding control error vector

$$\boldsymbol{\varepsilon}(t) = z(t) - y(t) = (q^{-d}\boldsymbol{D} - \boldsymbol{\mathscr{H}}\boldsymbol{\mathscr{R}}_p) r_p(t+d) \ .$$

The control paths $\boldsymbol{\mathscr{H}}\boldsymbol{\mathscr{R}}_p$ are here made to approximate the desired impulse response matrix $q^{-d}\boldsymbol{D}(q^{-1})$. Increasing the delay in any row vector of $\boldsymbol{D}(q^{-1})$, increases the approximation fidelity of the solution corresponding to that vector, approaching the noncausal Wiener solution as the delay tends to infinity. We have, in our experiments, used a rather long delay of 0.2 s as a musical input signal will be fairly insensitive to such delays. We have also restricted the experiments to the case $L = 1$ and $g = 1$. If latency sensitive (e.g. phone call) functionality is to be incorporated in the system it is recommendable to include such a signal in $r_p(t)$ and to set a shorter delay in the corresponding row vector of $\boldsymbol{D}(q^{-1})$. This results in a reduced quality sound reproduction and possibly more leakage of the telephone calls into the other zones as compared to the music signal but with the crucial benefit of reduced latency.

The feedforward regulator is designed to minimize the scalar quadratic criterion

$$J \quad = \quad E\{(\boldsymbol{V}\boldsymbol{\varepsilon}(t))'\boldsymbol{V}\boldsymbol{\varepsilon}(t) + (\boldsymbol{W}u(t))'\boldsymbol{W}u(t)\} \tag{5}$$

under constraints of stability and causality of $\boldsymbol{\mathscr{R}}_p(q^{-1})$ [1] The expectation $E(\cdot)$ in (5) is taken with respect to the statistical properties of $r_p(t)$. The weighting $\boldsymbol{V}(q^{-1})$ is a square polynomial matrix of full rank M. The square polynomial matrix $\boldsymbol{W}(q^{-1})$ can be used to focus the control energy into frequency ranges that are appropriate for particular loudspeakers and to avoid non-favourable linear combinations of loudspeakers.

2.3. The LQG Feedforward Controller

Formulating the MIMO LQG feedforward controller described above is possible if there exists an $N \times N$ polynomial matrix $\beta(q^{-1})$ that satisfies the spectral factorization equation

$$\beta_*\beta = \boldsymbol{B}_*\boldsymbol{V}_*\boldsymbol{V}\boldsymbol{B} + \boldsymbol{A}_*\boldsymbol{W}_*\boldsymbol{W}\boldsymbol{A} \ . \tag{6}$$

The polynomial matrix $\beta(q^{-1})$ described in (6) is guaranteed to exist and to be stably invertible under mild conditions, for example by the use of a control signal penalty matrix $\boldsymbol{W}$ such that $\det[\boldsymbol{W}(z^{-1})] \neq 0$ on the unit circle $|z| = 1$. Given $\beta(q^{-1})$, the unique stable linear feedforward controller that minimizes (5) for a model (1), (2), (3) can be computed by

$$u(t) = \boldsymbol{\mathscr{R}}_p(q^{-1})\, r_p(t+d) = \boldsymbol{A}\,\beta^{-1}\boldsymbol{Q}\, r_p(t+d) \ . \tag{7}$$

The $N \times L$ polynomial matrix $\boldsymbol{Q}$ is found together with the noncausal $N \times L$ polynomial matrix $\boldsymbol{L}_*$ as the unique solution to the linear polynomial matrix equation (Diophantine equation)

$$q^{-d}\boldsymbol{B}_*\boldsymbol{V}_*\boldsymbol{V}\boldsymbol{D} = \beta_*\boldsymbol{Q} + q\boldsymbol{L}_*\boldsymbol{H} \ . \tag{8}$$

See Section 3.3 of [7] for a proof.

The controller can now be found by combining (6) and (8). Both of these equations can be efficiently solved by

[1] The regulator is restricted to be "causal" in the sense that it does not utilize $r_p(t+k)$ for $k > d$.

existing techniques. See e.g. [12] for an overview of the spectral factorization problem.[2]

The controller $\mathscr{R}_p(q^{-1})$ in (7) is a matrix of high-order IIR filters with L inputs and N outputs. Since this filter is to be implemented with finite precision arithmetic, it is approximated by a high order FIR filter in the experiments described below.

The total control signal vector $\bar{u}(t)$ to the N loudspeakers is generated as the sum of the g individual acoustic zone control signals

$$\bar{u}(t) = \sum_{p=1}^{g} \mathscr{R}_p(q^{-1}) r_p(t+d). \tag{9}$$

2.4. Soundfield Complexity

The spatial complexity of a soundfield is strongly frequency dependent. For low frequencies, the wavelengths are long and only a limited number of periods may be fitted in a closed space such as e.g. the interior of a car. This in turn means that the space dependent magnitude and phase of a low frequency wave has a limited rate of change over a volume of space. For increasing frequencies and decreasing wavelengths, the variability of gain and phase over space increases. The practical implications of this is that there is an upper limiting frequency where we can not expect to be able to control a soundfield with the available set of loudspeakers. For a more detailed discussion on the concept of soundfield dimensionality and the limits on soundfield reproduction imposed by this, see e.g. [4] and Ch. 3 of [8].

3. EXPERIMENTAL EVALUATION

3.1. Experimental Setup

All experiments described in this paper were carried out in a common series-production car equipped with nine high-end speakers native to the car, see Fig. 1. The car was equipped with two subwoofers, located under the front seats, and seven mid-range speakers. An additional subwoofer was also placed in the trunk of the car. The transfer functions from each speaker to the listener positions were measured in four (one per seat)

[2]The general solution outlined in [7] also requires the solution of polynomial matrix coprime factorizations, and sometimes an extra Diophantine equation. With the model parametrization used here, with FIR models in (2) and stable AR models in (3), no coprime factorizations or extra Diophantine equations are needed.

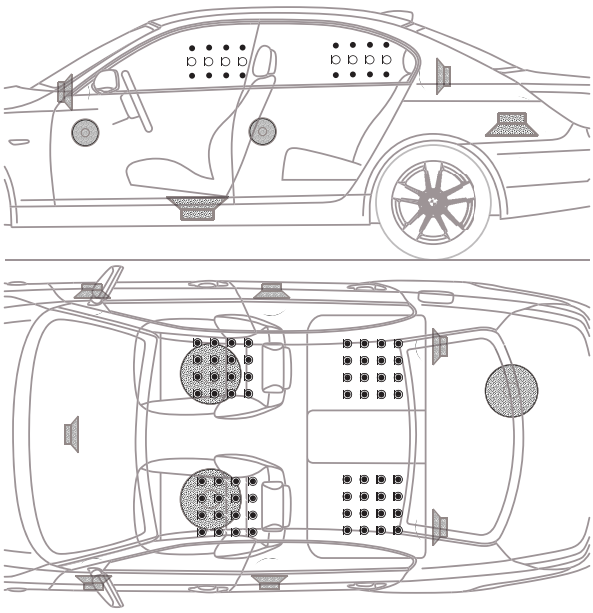

Fig. 1: Setup of the bass- and mid-range loudspeakers and the microphone positions in the car. All loudspeakers except the subwoofer in the trunk are the built-in loudspeakers. The '○' symbols represent the microphone positions for design measurements, and the small '•' symbols represent the additional positions where verification measurements were performed.

0.3×0.3 m grids at ear height of the potential listeners using four calibrated omnidirectional microphones. The measurements were done using a chirp signal with a gain tuned for good SNR without unnecessarily exciting any non-linearities of the system. These grids constitute the groups as discussed in Section 2 and the front left seat grid was designated the 'target grid', G_T, throughout the experiments and simulations described below. The microphone separation within each grid was 0.1 m yielding a total of 16 (4×4) measurement positions per group. Additional grids were measured at 0.1 m above and below the ear-height grids to be used for evaluation of the vertical variance of the solution. As the solution is expected to deteriorate for higher frequencies and the filters easily have impulse response lengths of more than half a second, the filters were designed for a sampling rate of 3200 Hz. This suffices in order to cover the highest frequency where the solution is effective while keeping the computational complexity at manageable levels.

The design and evaluation procedure was as follows: First, all transfer functions of a signal path, from the dig-

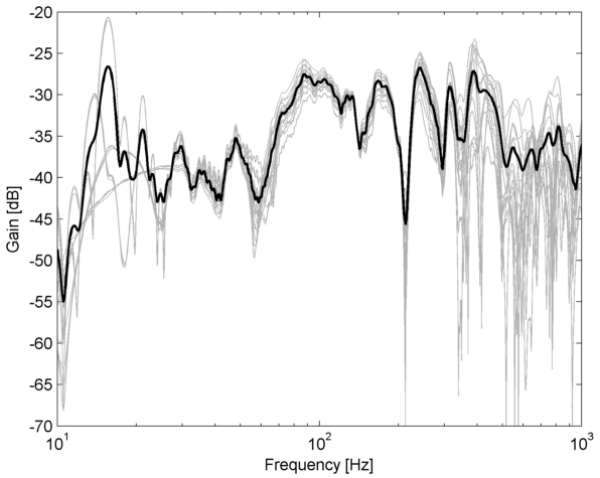

Fig. 2: Power gain in dB versus frequency of the loudspeaker-microphone system considering one of the two subwoofers and the driver's seat grid. The thicker middle line is the mean over the grid while the thinner lines are the individual microphones. The curve is clearly dominated by measurement noise up to 30 Hz and the loudspeaker is able to output power well above 500 Hz.

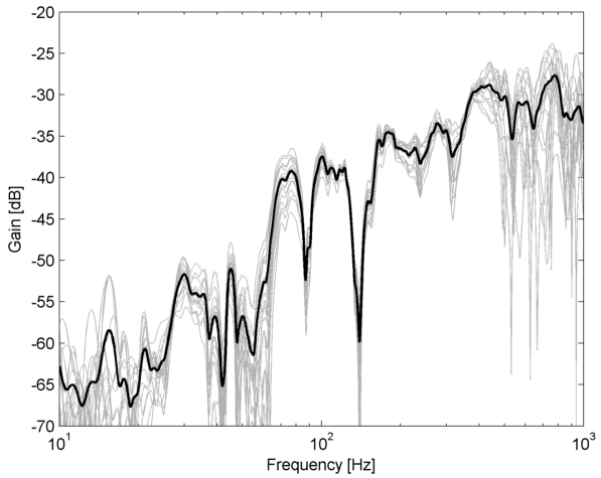

Fig. 3: Power gain in dB versus frequency of the loudspeaker-microphone system considering one of the seven mid-range speakers and the driver's seat grid. The thicker middle line is the mean over the grid while the thinner lines are the individual microphones. The speaker outputs significant power from about 60 Hz up to at least 1 kHz where the soundfield is of such complexity that we can not hope to control it with our nine speakers.

ital representation in a computer via the soundcard, amplifiers, loudspeakers and microphones were measured at all design positions (◯ in Fig. 1). Secondly, a controller aiming at a flat spectrum and unit gain for the driver's seat (front left) microphone group, G_T, and zero gain for the other microphone groups was designed. Only the built-in speakers were used in the controller design on which the experiments are based. The controller was designed for the case $L = 1$, prompting $\boldsymbol{D}(q^{-1})$ of (2) to be a row vector. Further, the target delay of $\boldsymbol{D}(q^{-1})$ was chosen to be equal over the whole target group meaning that no particular direction of sound wave propagation was implemented in the design on which the experiments were based. Controller performance was then evaluated by estimating the transfer function of the system with the controller in the loop. Finally, the actual attenuation at the zero gain measurement positions was measured by playing a white noise through the system and comparing the power levels at the zero gain groups to that of the unit gain target group. This was also done for the higher and lower validation grids ('•' in Fig. 1).

In the filter design phase, the control signal penalty matrix $\boldsymbol{W}$ of (5) was chosen diagonal, with FIR filters on its diagonal. These filters were adjusted in such a way that the two subwoofers were allowed to output energy in the frequency range 20–220 Hz. The mid-range speakers were limited to the range 60–800 Hz. These choices were motivated by the loudspeakers' respective power spectral density curves (Fig. 2 and Fig. 3) and the upper frequency limit of where we do not expect any improvement from the compensation (note how the power curves at the different microphone positions deviate above 400 Hz and see Section 2.4). The lower limit is a safeguard so as to not set high gains of the filter in regions where the signal to noise ratio of the identification measurements is poor. Looking closer at the loudspeaker response curves, the subwoofer shows clear signs of identification measurement noise below 30 Hz and a wiser choice of lower limiting frequency may be 30 Hz. Admittedly, the subwoofers may be used above 220 Hz and were so in the simulations described below.

Both the measured design and the design evaluated solely by simulations were intended for a musical input signal and were therefore allowed the rather long delay d in (2) of 0.2 s. A simulation based investigation was undertaken in order to see what can be achieved if the number of loudspeakers with low frequency capabilities is increased. The extra loudspeaker in the trunk is here used to achieve an additional degree of freedom. In this

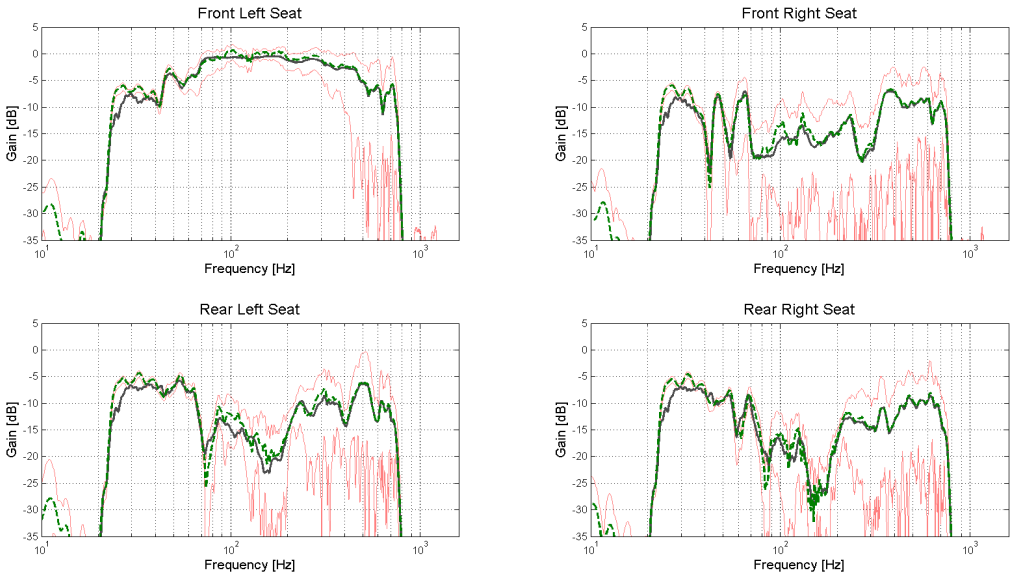

Fig. 4: Reslut of system identification of the controlled system, which targets a flat frequency response at the front left seat and silence at all other. The thick dashed (green) line is the measured result, the thick (gray) full line is the expected result from a simulation. Both the result and the simulation are mean values over the respective groups. The thinner lines show the maximum and minimum gain at any measurement point in each group.

investigation, the lower frequency limits of the built-in subwoofers were adjusted to 30 Hz and the upper limits to 800 Hz in compliance with Fig. 2. The added subwoofer has a more pronounced low frequency characteristic and was used between 30 and 300 Hz. In the simulation, a scalar input $r(t)$ was used and a target stage vector $\boldsymbol{D}(q^{-1})$, representing a plane wave moving from the front end to the rear end of G_T, was set. This was intended to produce a virtual plane-wave source straight in front of the driver. This simulation is the only instant where the trunk subwoofer was utilized.

3.2. Experimental Results

The results from the system identification, where the transfer functions (from system input to system output of loudspeakers, microphones, car interior and electronic equipment) after compensation were investigated, are shown in Fig 4. A simulation of the same setup and system as the experiments are based on is also shown in Fig. 4 for comparison. The figure shows the per-frequency power gain of each zone (or seat as the zones are designed around the seats of the car). We see in Fig. 4 that an average power difference in excess of 10 dB between the targeted seat and any other seat in the frequency range 70–200 Hz is achieved. Above 200 Hz, there is also substantial attenuation as far up as 500 Hz for the rear right and front right seat. There is very little difference in sound pressure below 70 Hz. This is due to the fact that a system with only two subwoofers simply lacks the necessary degrees of freedom to independently control four different zones. It can be noted that there are some deviations between the simulated result and the actual measured result of Fig. 4. Knowing that four microphones were used to measure the responses by repeating a test sequence and moving the microphones, there are some conclusions that may be drawn about these deviations. Primarily, the bumps around 30 Hz appear in all four seats. This means that they are present in several measurements done over a long (several minutes) period of time. It is therefore plausible that the error stems from modeling errors rather than noise in the verification measurements. In general, deep notches in the response seem to be hard to model and predict accurately. There is also a zone between (roughly) 90 and 300 Hz with reduced

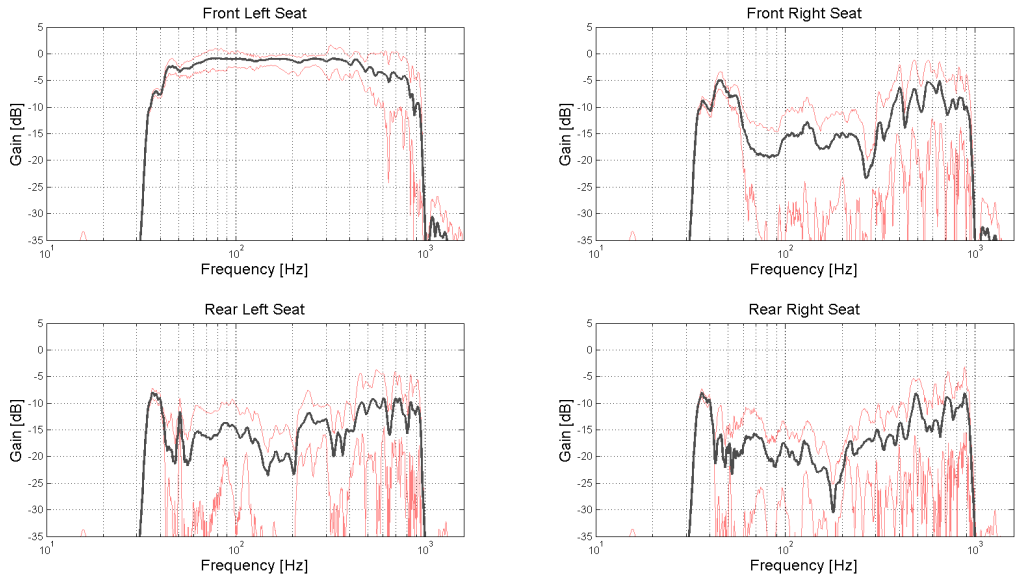

Fig. 5: Simulation of system response using the additional trunk subwoofer. The thick (gray) full line shows the mean simulated responses of the system. The thinner lines show the simulated maximum and minimum gain of any measurement point in each group.

simulation accuracy. These deviations do not, however, interfere much with the conclusions that may be drawn from the simulated results.

In Fig. 5, a simulation where the additional subwoofer located in the trunk of the car is used to support the two built in subwoofers is shown. Here we see that the poor performance in the low frequency regions is almost completely resolved and a zoning effect may be discerned all the way down to 40 Hz after which the filter gains decreases quickly, due to the control penalty filter $\boldsymbol{W}$ used in the design, in order to reach zero at 30 Hz. No drastic negative effects of the changed target delay relationship can be discerned in the figure, indicating that there is room for acoustic profiling in the zone design.

The result of the random noise signal played through the controller is shown in Fig. 6 for the ear height measurements. These are the measurement positions on which the controller design was based. The figure shows the difference in mean squared sound pressure between the target group (driver's seat) and the other groups (seats) plotted against frequency. We see, again, a substantial difference between the zones in the range 70–400 Hz. A similar plot depicting the results of the measurements at the higher validation measurement grid is found in Fig. 7. Although some deterioration of the sound pressure differences can be observed compared with the ear-height measurements for which the controller was designed, the differences between the zones are still mostly greater than 10 dB from 70–400 Hz. The lower grid measurements display similar trends, indicating a significant robustness of the solution with respect to vertical displacements.

4. CONCLUSIONS

This paper has shown that sound of frequencies in the approximate range 70–400 Hz may be successfully divided into four zones using a multipoint MSE based controller design. It has also been shown that with our setup, the lower limit on this range may be pushed to the limits of the loudspeakers' performance by increasing the number of subwoofers from two to three. The control strategy has also been shown to be robust with respect to variations in the vertical dimension. The robustness of the design with respect to variations in the transfer functions due to e.g. changes in passenger constellations has

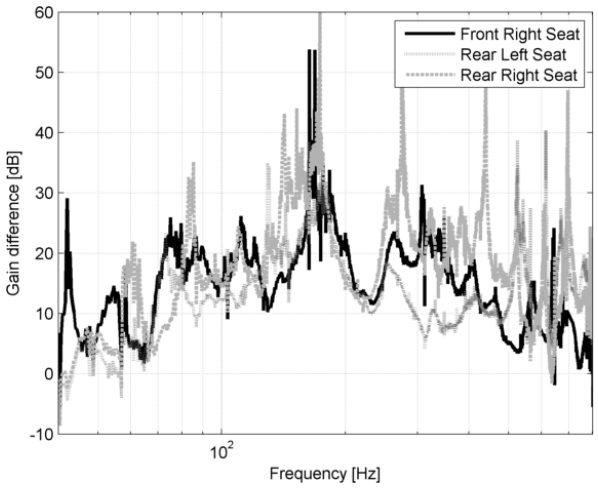

Fig. 6: Difference in mean squared sound pressure [dB] between the driver's seat and the other seats at ear height of a noise fed through the compensated system. The full line is compared to the front right seat, the dotted line is compared to the rear left seat and the dashed line is compared to the rear right seat.

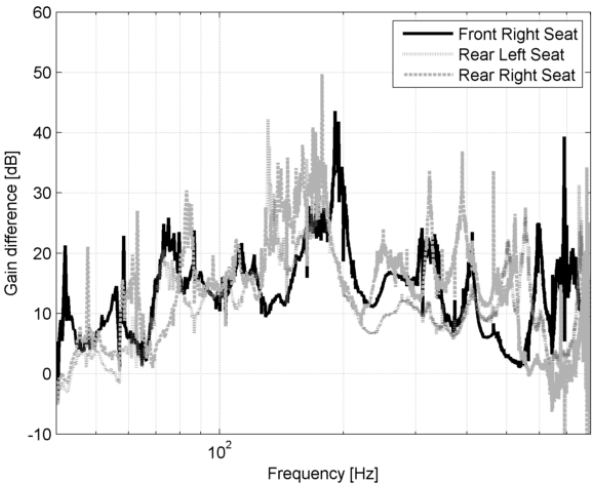

Fig. 7: Difference in mean squared sound pressure [dB] between the driver's seat and the other seats about 0.1 m above ear height of a noise fed through the compensated system. The full line is compared to the front right seat, the dotted line is compared to the rear left seat and the dashed line is compared to the rear right seat.

not been investigated but is left for future works.

This work takes a somewhat different approach to a similar problem described in [1]. It is intended as a partial solution for a system with both global sound system speakers and local speakers for control at higher frequencies. The intended local speakers solution is in essence comparable to the work presented in [3] but is not investigated in this paper.

5. REFERENCES

[1] Y. J. Wu and T. D. Abhayapala, "Spatial Multizone Soundfield Reproduction: Theory and Design," *IEEE Transactions on Audio, Speech, and Language Processing,* vol. 19, no. 6, August 2011.

[2] A. J. Hill and M. O. J. Hawksford "Individualized low-frequency response manipulation for multiple listeners using chameleon subwoofer arrays" *3rd Computer Science and Electronic Engineering Conference (CEEC)*, Colchester, UK, July 13–14 2011.

[3] M. Jones and S. J. Elliot, "Personal audio with multiple dark zones," *J. Acoust. Soc. Am.* Volume 124, Issue 6, pp. 3497–3506 (2008).

[4] R. A. Kennedy, P. Sadeghi, T. D. Abhayapala and H. M. Jones, "Intrinsic Limits of Dimensionality and Richness in Random Multipath Fields," *IEEE Transactions on Signal Processing,* vol. 55, no. 6, pp. 2542–2556 (June 2007).

[5] A. Ahlén and M. Sternad, "Wiener filter design using polynomial equations," *IEEE Transactions on Signal Processing*, vol. 39, pp. 2387–2399, 1991.

[6] T. J. Sutton, S. J. Elliott, A. M. McDonald and T. J. Saunders, "Active noise control of road noise inside vehicles," *Noise Control Engineering Journal*, vol. 42, pp. 137–147, July–Aug. 1994.

[7] M. Sternad and A. Ahlén, LQ Controller Design and Self-tuning Control. Chapter 3 in K. Hunt Ed, *Polynomial Methods in Optimal Control and Filtering*, Control Engineering Series, Peter Peregrinus, London, Jan. 1993, pp. 56–92.

[8] L-J Brännmark, *Robust Sound Field Control for Audio Reproduction: A Polynomial Approach to Discrete-Time Acoustic Modeling and Filter Design.* Ph.D Thesis, Dept. of Engineering Sciences, Uppsala University, January 2011.

[9] M. Johansson, L.-J. Brännmark, A. Bahne and M. Sternad, "Sound field control using a limited number of loud-

speakers," *AES 36th International Conference*, Dearborn, Michigan, US, June 2–4 2009.

[10] S. Berthilsson, A. Barkefors and M. Sternad, "MIMO Design of Active Noise Controllers for Car Interiors: Extending the Silenced Region at Higher Frequencies," *American Control Conference*, Montréal, Canada, June 27–29 2012.

[11] T. Kailath, *Linear Systems*, Prentice-Hall, Englewood Cliffs, New Jersey, 1980.

[12] V. Kŭcera, "Factorization of rational spectral matrices: a survey of methods," *IEE Control 91*, Edinburgh, pp. 1074–1078, 1991.